Synthesis and Structural Characterization of Five Layer Copper Titanium Oxide Perovskites

Maria J. Pack, Anne Gormezano, and Mark T. Weller*

Department of Chemistry, The University of Southampton, Highfield, Southampton, SO17 1BJ, UK

Received November 6, 1996. Revised Manuscript Received February 25, 1997[⊗]

The synthesis and characterization of six members of the ordered quintuple copper titanium perovskite series $Ln_2Ba_2CaCu_2Ti_3O_{14}$ are reported. Structural characterization, carried out by a combination of powder X-ray and powder neutron diffraction and EXAFS, shows full ordering of the cations for Ln = Sm, Eu, Gd in the tetragonal space group *P*4/*mmm* with the B type cations stacked in the order Cu−Ti−Ti−Ti−Cu. For Ln = Nd partial disorder on both the A and B cation sublattices occurs and oxygen is incorporated between the CuO_2 layers. In $La_2Ba_2CaCu_2Ti_3O_{14}$ there is full disordering on both the A and B cation lattices leading to a simple cubic unit cell. When Ln = Tb and Dy, the symmetry of the structure is reduced to an orthorhombic cell, though the B cation stacking is maintained. In all materials the TiO_6 octahedra are distorted. The in-plane Cu−O distances are similar to those found in high-temperature superconductors and are significantly shorter than those found in the corresponding quadruple copper titanium lanthanide perovskites.

Introduction

Complex oxide structures containing cuprate layers formed from linked CuO_4 square planes, CuO_5 square pyramids, or CuO_6 octahedra are of considerable interest in terms of their electronic properties and specifically superconductivity. All of these superconducting cuprates have structural elements that may be considered to be derived from the perovskite structure. Structural complexity may be considered to be increasing as the number of perovskite blocks (which may be oxygen deficient) involved in the formation of the unit cell increases. For example, in the series of compounds Ba_2InCuO_4,[1] $YBa_2Cu_3O_7$,[2] $Gd_2Ba_2Ti_2Cu_2O_{11}$,[3] and $SrCuO_2$[4,5] the number of perovskite cubes stacked to form the unit cell may be considered to be 2, 3, 4, and infinity, respectively.

The quadruple perovskite structure was first reported for $La_2Ba_2Sn_2Cu_2O_{11}$[6] where the B cations forming the perovskite blocks are ordered in layers as [Cu−Sn−Sn−Cu]. The large size of tin relative to copper leads to considerable mismatch between the layers and lengthening of the Cu−O bonds. In $Gd_2Ba_2Ti_2Cu_2O_{11}$[3] the smaller titanium ion allows reduction of the copper−oxygen distances to more typical values close to 1.96 Å though distortions still occur in the TiO_6 octahedra.

New layered cuprate oxides containing Ti(IV) and Cu(II) can be prepared by addition of further structural units into the basic quadruple perovskite unit cell. The introduction of an additional $CaTiO_3$ perovskite layer into the $Ln_2Ba_2Ti_2Cu_2O_{11}$ phase was first reported by Zhu et al.[7] in $Sm_2Ba_2CaCu_2Ti_3O_{14}$. The structure of this compound can be viewed as the intergrowth of two layers formed from copper−oxygen square pyramids and three titanium-based perovskite layers. Its structure is shown in Figure 1, and its atom stacking sequence along the *c* axis can be described as

$$Ca-[CuO_2]-BaO-[TiO_2]-SmO-[TiO_2]-SmO-[TiO_2]-BaO-[CuO_2]$$

Perovskites containing TiO_6 octahedra often show distortions in terms of the positions of oxide and titanium ions, and these distortions are often responsible for the ferroelectric properties associated with phases of this type. Ferroelectric effects are seen in compounds such as $BaTiO_3$,[8] $Bi_4Ti_3O_{11}$,[9] and $Bi_2TiO_4F_2$[10] with marked displacements of the titanium atom within the TiO_6 octahedron. In the quadruple layer perovskites such as $Gd_2Ba_2Ti_2Cu_2O_{11}$ distortions of the TiO_6 octahedra occur and are thought to be associated with a mismatch between the titanium oxide and copper oxide layers, though the origin may actually be the dislike of Ti^{4+} of regular octahedral geometry.

This paper reports the introduction of different A cations into the quintupled perovskite structure first described by Zhu et al.[7] and the effect of an additional perovskite layer on the polyhedral tilt in the structure. The true oxygen distributions are determined, and the formation of this phase using Goldschmidt tolerance

[⊗] Abstract published in *Advance ACS Abstracts,* June 1, 1997.

(1) Kharlanov, A. L.; Khasanova, N. R.; Paromova, M. V.; Antipov, E. V.; Lykova, L. N.; Kovba, L. M. *Russ. J. Inorg. Chem.* **1990**, *35*, 3067.

(2) Wu, M. K.; Torng, C. J.; Meng, R. L.; Gao, L.; Huang, Z. J.; Wang, Y. Q.; Chu, C. W. *Phys. Rev. Lett.* **1987**, *58*, 909.

(3) Gormezano, A.; Weller, M. T. *J. Mater. Chem.* **1993**, *3*, 771. Gormezano, A.; Weller, M. T. *Chem. Mater.* **1995**, *7*, 1625.

(4) Teske, C. L.; Müller-Buschbaum, H. K. *Z. Anorg. Allg. Chem.* **1970**, *379*, 234.

(5) Yamane, H.; Miyazaki, Y.; Hirai, T. *J. Chem. Soc. Jpn. Int. Ed.* **1989**, *97*, 140.

(6) Anderson, M. T.; Poeppelmeier, K. R.; Zhang, J. P.; Fan, H. J.; Marks, L. D. *Chem. Mater.* **1992**, *4*, 1305.

(7) Zhu, W. J.; Huang, Y. Z.; Ning, T. S.; Zhao, Z. X. *Mater. Res. Bull.* **1995**, *30*, 243.

S0897-4756(96)00575-3 CCC: $14.00

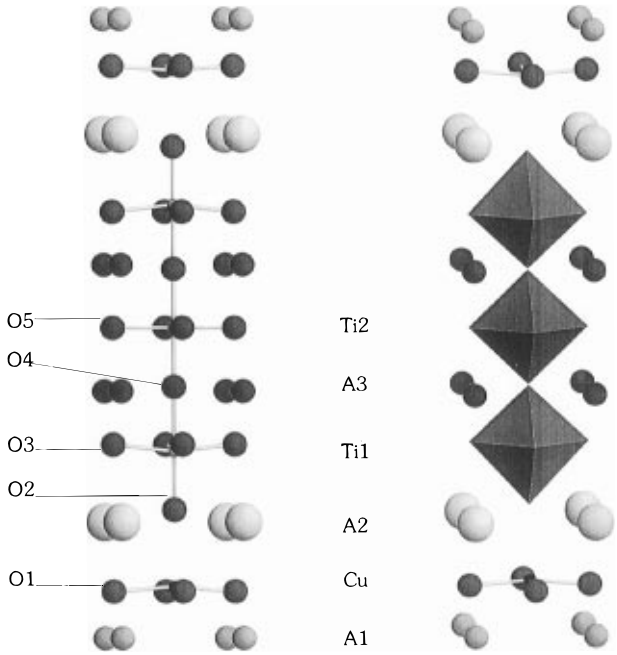

Figure 1. Quintupled perovskite structure of $Ln_2Ba_2CaCu_2Ti_3O_{14}$. The idealized structure, with regular TiO_6 octahedra and CuO_5 square pyramids, is shown.

factors,[11] with ionic radii data taken from Shannon,[12] has been rationalized.

Experimental Procedure

Synthesis. Stoichiometric amounts of Ln_2O_3 (99.9%), $BaCO_3$ (99.5%), $CaCO_3$ (99%), CuO (99.95%), and TiO_2 (99%) were thoroughly mixed, ground, and initially heated at 950 °C in order to decompose the carbonates. The resulting mixture of oxides was then pelletized and heated at 1025 °C for 48 h with intermediate regrinding. The phase obtained was further oxygen annealed at 1000 °C for 24 h and furnace cooled to room temperature to ensure full oxygen occupancy. A summary of the targeted phases and the resulting products, as determined from powder X-ray and powder neutron diffraction data, is given in Table 1. Tolerance ratios for each of the targeted compositions were calculated using the procedure reported by Anderson et al.[13] Attempts to synthesize $Ho_2Ba_2CaCu_2Ti_3O_{14}$ produced multiphase products.

Samples were also required for neutron diffraction experiments but naturally occurring samples of gadolinium and samarium oxides contain the highly absorbing isotopes (^{157}Gd and ^{149}Sm), and for these reasons samples containing only ^{160}Gd and ^{154}Sm were synthesized. The isotopes were extracted from the quadrupled perovskite samples previously used for neutron diffraction experiments[3] by dissolution in 2 M nitric acid, electrodeposition of copper, and precipitation of the lanthanide oxalate; the oxalate was converted to the oxide through decomposition at 900 °C. Quintupled perovskite samples containing the nonabsorbing isotopes were synthesized from the oxides as described above.

Structure Refinement. Initial structural characterization was carried out by Rietveld refinement of powder X-ray diffraction data. Data were collected for all samples (Ln = La, Nd, Sm, Eu, Gd, Tb, and Dy) on a Siemens D5000 diffractometer operating with Cu $K_{\alpha 1}$ radiation over a period of 15 h. All the data sets, except Ln = La, were indexed using a tetragonal perovskite unit cell with $c \approx 5a_p$ and space group *P*4/*mmm* as indicated by the systematic absences observed in the pattern, though peak widths for some reflections in the profile of the terbium and dysprosium samples indicated the possibility of a cell distortion (vide infra). Data from the Ln = La samples could be indexed on a simple cubic perovskite unit cell of dimension 3.9447(5) Å.

Structure refinement of $Eu_2Ba_2CaCu_2Ti_3O_{14}$ using the powder X-ray diffraction data was undertaken using the GSAS Rietveld refinement package,[14] and the data published for $Sm_2Ba_2CaCu_2Ti_3O_{14}$[7] were used as a starting model. The A2 (0.5,0.5,*z*), $z \approx 0.19$ site, which separates the copper and titanium layers, was assumed to be solely occupied by the barium cations, as is the case for the similar site in the quadrupled perovskite phases, $Ln_2Ba_2Ti_2Cu_2O_{11}$. A mixture of europium and calcium was statistically allocated to the A1 (0.5,0.5,0.0) and A3 (0.5,0.5,*z*), $z \approx 0.4$ cation sites in the initial stages of the refinement, but the site occupancies were allowed to vary within the compound stoichiometry in later cycles. The refined occupancy values were very close to the initial occupancies and were therefore set at these values in the initial stages of the refinement. The preliminary cycles of the refinement placed oxide ions on the special sites used by Zhu et al.[7] with individual positional parameters refined where possible. A single, refined temperature factor was used for all these sites in the early stages of the refinement, but crystallographically different sites were permitted individual, refined temperature factors at a later stage of the refinement process. The *B* values obtained were reasonable for all sites except O4 (0.0,0.0,*z*), $z \approx 0.4$ and O5 (0.0,0.5,0.5) where site values of 11 and 9 Å^2 were generated, indicating that the true scattering density was poorly modeled in both cases by a single-site model. However, with powder X-ray diffraction data no stable refinements with oxygen displaced off these special sites could be undertaken.

Final stages of the refinement involved approximately 30 parameters including scale factor, background, peak shape, unit cell, and positional parameters. Isotropic thermal factors were refined for all sites. The final profile fit to the powder pattern for $Eu_2Ba_2CaCu_2Ti_3O_{14}$ can be seen in Figure 2. Results, final refined atomic positions and temperature factors, for the europium sample is summarized in Table 2 and derived bond lengths and angles given in Table 6. The refinements for the other lanthanide derivatives were carried out in an analogous fashion. For Ln = Nd, Sm, and Gd refinement was completed in the space group *P*4/*mmm*. However, the profile fits obtained for $Tb_2Ba_2CaCu_2Ti_3O_{14}$ and $Dy_2Ba_2CaCu_2Ti_3O_{14}$ were relatively poor, and close inspection of the peak profiles indicated that the individual peaks were poorly modeled by the tetragonal symmetry. The structures of these compounds were therefore refined using an orthorhombically distorted unit cell as determined from the high-resolution neutron data for $Dy_2Ba_2CaCu_2Ti_3O_{14}$ (vide infra). The structural results obtained for $Tb_2Ba_2CaCu_2Ti_3O_{14}$, using an ordered oxide model, are summarized in Table 3, and derived bond lengths and angles, for this compound, in Table 6.

The accurate definition of oxygen atom positions and the determination of the distribution of near isoelectronic species (Ba/Ln and Cu/Ti) is impossible from powder X-ray diffraction data. For this reason further structural analysis was performed using high-resolution neutron diffraction data. Powder neutron diffraction data were collected for $Ln_2Ba_2CaCu_2Ti_3O_{14}$ where Ln = Nd, ^{154}Sm, ^{160}Gd, and Dy, on the high-resolution powder diffractometer (HRPD) on ISIS at the Rutherford Appelton Laboratory. Samples of mass ~2 g were loaded in vanadium cans and backscattered data collected at the 1 m position over the time-of-flight (TOF) range 30 000−130 000 μs. Data were collected at room temperature for approximately 10 h. The Rietveld refinements were carried out using the GSAS package[14] with neutron scattering lengths and absorption cross-sections taken from Jacobson et al.[15]

(8) Smolenskii, G. A. *Zh. Tekh. Fiz.* **1950**, *20*, 137.
(9) Aurivillius, B. *Ark. Kem.* **1949**, *58*, 499.
(10) Aurivillius, B. *Ark. Kem.* **1952**, *5*, 39.
(11) Goldschmidt, V. M. *Str. Ner. Vidensk-Akad Oslo* **1926**, *1*, 1.
(12) Shannon, R. D. *Acta Crystallogr.* **1976**, *32A*, 751.
(13) Anderson, M. T.; Poeppelmeier, K. R. *Chem. Mater.* **1991**, *3*, 476.
(14) GSAS; Larsen, A. L.; von Dreele, R. B. MS-H805, Los Alamos National Laboratory.
(15) Jacobson, A. G.; Totfield, B. C.; Fender, B. E. F. *J. Phys. Chem.* **1975**, *6*, 1625.

Table 1. Phase Behavior in the System $Ln_2Ba_2CaCu_2Ti_3O_{14}$

stoichiometry	obtained phase	tolerance factor	a (σa) (Å)	c (σc) (Å)
$La_2Ba_2CaCu_2Ti_3O_{14}$	disordered perovskite	0.990	a = 3.9447(5)	
$Nd_2Ba_2CaCu_2Ti_3O_{14}$[a]	ordered five layer perovskite	0.977	3.9036(1)	19.619(1)
$Sm_2Ba_2CaCu_2Ti_3O_{14}$[a]	ordered five layer perovskite	0.973	3.8921(2)	19.583(1)
$Eu_2Ba_2CaCu_2Ti_3O_{14}$	ordered five layer perovskite	0.971	3.8818(4)	19.572(2)
$Gd_2Ba_2CaCu_2Ti_3O_{14}$[a]	ordered five layer perovskite	0.969	3.8788(1)	19.580(1)
$Tb_2Ba_2CaCu_2Ti_3O_{14}$	ordered five layer perovskite	0.968	a =5.4667(4) b =5.4820(4)	19.556(1)
$Dy_2Ba_2CaCu_2Ti_3O_{14}$[a]	ordered five layer perovskite	0.967	a =5.4825(2) b = 5.4617(2)	19.569(2)

[a] PND data. All others from Rietveld refinement of powder X-ray diffraction data.

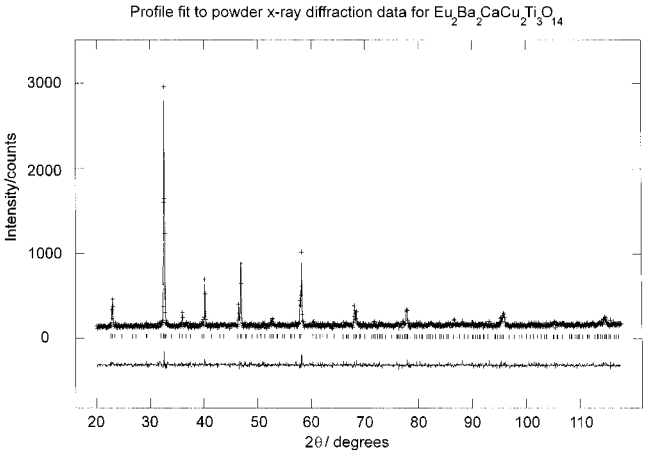

Figure 2. Fit to the powder X-ray diffraction data for $Eu_2Ba_2CaCu_2Ti_3O_{14}$. Experimental data points are shown as crosses, calculated profile the upper continuous line, and difference profiles as the lower continuous line. Tick marks show reflection positions.

Table 2. Refined Parameters from Powder X-ray Diffraction Data of $Eu_2Ba_2CaCu_2Ti_3O_{14}$[a]

atom	x	y	z	B/Å^2	occupancy
Eu(1)	0.5	0.5	0	0.6(4)	1.0
Ba	0.5	0.5	0.1879(4)	2.4(3)	1.0
Ca/Eu(3)	0.5	0.5	0.3979(6)	1.3(3)	0.5/0.5
Cu	0.0	0.0	0.0855(7)	1.1(5)	1.0
Ti(1)	0.0	0.0	0.3005(11)	1.7(6)	1.0
Ti(2)	0.0	0.0	0.5	0.6(9)	1.0
O1	0.0	0.5	0.0784(17)	1(1)	1.0
O2	0.0	0.0	0.2040(32)	3(2)	1.0
O3	0.0	0.5	0.3093(25)	3(2)	1.0
O4	0.0	0.0	0.4051(51)	11(3)	1.0
O5	0.0	0.5	0.5	9(4)	1.0

[a] Space group $P4/mmm$ a = 3.8818(4), c = 19.5724(19) Å. R_{wp} = 8.21. R_{exp} = 2.52.

The model used in the refinement was based on structural details obtained through the PXD studies on these materials with space group $P4/mmm$ and lattice parameters and atomic coordinates were taken from the final cycles of this analysis. The initial stages of the refinement included overall scale factors, background, lattice parameters, peak shape parameters, and isotropic thermal parameters. On refinement the isotropic temperature factors of the O4 and O5 sites were again relatively high and refinements of the anisotropic temperature factors for these sites suggested displacement of O4 from a 2g (0,0,z) site to an 8r (x,x,z) site, and similar displacement from the x-axis for the O5 site to a 4o (x,0.5,0.5) site. These atoms were therefore allowed to move on to these sites with partial occupancy reflecting a local oxygen level of unity. On refinement of atomic coordinates and thermal parameters the resulting isotropic temperature factor values were lower and chemically more sensible. The distribution of lanthanide, barium, and calcium ions over the three A cation sites present in the structure was also permitted to vary, together with site occupancies of the Cu and Ti sites in order to ascertain the completeness of cation ordering and true nature of layered

Table 3. Refined Parameters from Powder X-ray Diffraction Data of $Tb_2Ba_2CaCu_2Ti_3O_{14}$[a]

atom	x	y	z	B/Å^2	occupancy
Tb(1)	0.5	0	0	2.3(4)	1.0
Ba	0.5	0	0.1878(4)	2.1(3)	1.0
Ca/Tb(3)	0.5	0	0.3971(7)	1.8(4)	0.5/0.5
Cu	0	0	0.0834(9)	2.0(5)	1.0
Ti(1)	0.5	0.5	0.300(1)	1.2(7)	1.0
Ti(2)	0	0	0.5	2.5(1.3)	1.0
O1	0.25	0.25	0.076(2)	2.6(7)	1.0
O2	0	0	0.203(3)	2.6(7)	1.0
O3	0.25	0.25	0.308(3)	2.6(7)	1.0
O4	0.0	0.0	0.401(6)	12(3)	1.0
O5	0.25	0.25	0.5	12(3)	1.0

[a] Space group $Cmmm$ a = 5.4667(4), b = 5.4620(4), c = 19.556(1). R_{wp} = 9.60. R_{exp} = 2.93.

character of these materials. The incorporation of an oxygen between the CuO_5 pyramids was also considered and the occupancy of this site refined. For Ln = Nd, an oxygen atom on the 1a(0,0,0) has a refined site occupancy of 0.32(3), giving rise to an overall increased oxygen stoichiometry, $Nd_2Ba_2CaCu_2Ti_3O_{14.32}$.[16] Final stages of the refinement produced excellent fits to the data for the Ln = Nd, ^{154}Sm, and ^{160}Gd quintupled perovskites, though in the latter case two small regions containing weak impurity lines were excluded from the profile. The final profile fit obtained for $^{160}Gd_2Ba_2CaCu_2Ti_3O_{14}$ is shown in Figure 3. The determined atomic coordinates and temperature factors are summarized in Table 4; derived bond lengths and angles are given in Table 6. Calculated bond lengths for the interactions involving the oxide ions on disordered sites represent one possible set of distances.

For $Dy_2Ba_2CaCu_2Ti_3O_{14}$ a satisfactory fit to the profile in the $P4/mmm$ space group could not be achieved and close inspection of a number of reflections in the data set showed split peaks (Figure 4). Reindexing of the peaks could be achieved with an orthorhombic cell of approximate dimensions $\sqrt{2}a_p \times \sqrt{2}a_p' \times \simeq 5a_p$ where $a_p \simeq a_p'$. The coordinate system was reconfigured to this unit cell in the space group $Cmmm$; a similar distortion of a stacked perovskite cell is seen in the complex cuprate $Pb_2Sr_2YCu_3O_8$.[17] Refinement proceeded smoothly to convergence in this new orthorhombic description though as with the tetragonal unit cell it was necessary to locally distort the TiO_6 octahedra through displacements of the O3, O4, and O5 from the special sites. Temperature factors for (i) the B cations and (ii) the oxygen sites were constrained to a single value. Final refined atomic coordinates are summarized in Table 5 and derived bond distances given in Table 6.

EXAFS. EXAFS data were collected for the L III edge of gadolinium from $Gd_2Ba_2CaCu_2Ti_3O_{14}$ on Station 8.1 at the SRS Daresbury operating in transmission mode. Background subtraction was undertaken using PAXAS[18] and data analysis

(16) Gómez-Romero, P.; Palacin, M. R.; Rodriguez-Carvajal, J. *Chem. Mater.* **1994**, *6*, 2118.
(17) Cava, R. J.; Marezio, M.; Krajewski, J. J.; Peck Jr., W. F.; Santoro, A.; Beech, F. *Physica C* **1989**, *157*, 272.
(18) Binsted, N. PAXAS (Program for the Analysis of X-ray Absorption Spectra), University of Southampton, 1988.

Table 4. Refined Parameters from Powder Neutron Diffraction Data of $Ln_2Ba_2CaCu_2Ti_3O_{14}$ (Ln = Nd, Sm, Gd)[a]

Ln	*a*/Å	*c*/Å	Ln(1) *B*/Å^2	Ba/Ln(2) *z*	Ba/Ln(2) *B*/Å^2	Ca/Ln/Ba (3) *z*	Ca/Ln/Ba (3) *B*/Å^2	Cu *z*	Cu *B*/Å^2	Ti(1) *z*	Ti(1) *B*/Å^2	Ti(2) *B*/Å^2
Nd[b]	3.9036(1)	19.619(1)	0.59(20)	0.1919(3)	0.36(14)	0.3976(4)	0.26(19)	0.0834(8)	6.0(4)	0.3010(8)	6.0(4)	3.3(5)
Sm	3.8921(2)	19.583(1)	1.45(14)	0.1887(3)	0.33(13)	0.3980(2)	1.01(13)	0.0829(3)	2.27(21)	0.3035(11)	2.27(21)	3.7(4)
Gd	3.8788(1)	19.580(1)	0.39(8)	0.1873(2)	0.0(8)	0.3972(2)	1.25(9)	0.0837(2)	2.06 (10)	0.3000(5)	1.85(17)	1.49(26)

Ln	O1 *z*	O1 *B*/Å^2	O2 *z*	O2 *B*/Å^2	O3 *z*	O3 *B*/Å^2	O4 *x*	O4 *z*	O4 *B*/Å^2	O5 *x*	O5 *B*/Å^2	O6 *z*	O6 fraction	O6 *B*/Å^2
Nd	0.0855(3)	2.61(18)	0.2026(5)	3.13(26)	0.3048(4)	2.95(17)	0.0625(29)	0.3950(5)	1.77(50)	0.1076(26)	1.57(28)	0	0.323(34)	2.00
Sm	0.0792(2)	1.61(12)	0.2056(3)	2.44(17)	0.3109(3)	3.33(15)	0.0651(20)	0.4011(4)	1.61(37)	0.1044(18)	3.03(24)			
Gd	0.0761(15)	0.75(7)	0.2069(2)	1.62 (10)	0.3112(2)	3.80 (10)	0.0743(14)	0.4041(3)	1.50(26)	0.1140(17)	3.59(22)			

[a] Site positions and occupancies are as in Table 2, except for Nd (see fnt *b*), with only refined coordinates given. For O4 and O5 the refined sites were 8r (*x*,*x*,*z*) and 4o (x,$^1/_2$,$^1/_2$) with 0.25 and 0.5 occupancy. [b] For Nd the following cation distributions (esd's) were obtained Ba(2), 0.50(2)Ba + 0.50(2)Nd; Ca/La(3), 0.50(2)Ca + 0.5(2)Ba; Cu, 0.75(1)Cu + 0.25(1)Ti; Ti(1), 0.75(1) Ti + 0.25(1) Cu. Fit factors for Ln = Nd, Sm, Gd were R_{wp}/% = 8.20, 7.47, 6.35 and R_{exp}/% = 1.72, 2.92, 3.55, respectively.

Table 5. Refined Parameters from Powder Neutron Diffraction Data for $Dy_2Ba_2CaCu_2Ti_3O_{14}$[a]

atom	*x*	*y*	*z*	*B*/Å^2	occupancy
Dy(1)	0.5	0	0	0.03(15)	1.0
Ba	0.5	0	0.1880(4)	0.34(17)	1.0
Ca/Dy(3)	0.5	0	0.3972(3)	1.61(18)	0.5/0.5
Cu	0	0	0.0797(3)	1.28(19)	1.0
Ti(1)	0.5	0.5	0.3066(8)	1.28(19)	1.0
Ti(2)	0	0	0.5	1.28(19)	1.0
O1	0.25	0.25	0.0761(3)	0.21(13)	1.0
O2	0	0	0.2072(4)	0.21(13)	1.0
O3	0.2826(19)	0.2079(20)	0.3171(3)	0.21(13)	0.5
O4	0.023(4)	0.710(17)	0.4019(6)	0.21(13)	0.25
O5	0.3017(24)	0.1959(25)	0.5	0.21(13)	0.5

[a] Space group *Cmmm* a = 5.4825(2), b = 5.4617(2), c = 19.569(2).

carried out using EXCURV92.[19] Given the structural complexity of the system, particularly in view of the local distortion of the TiO_6 octahedra surrounding one of the two sites occupied by gadolinium, a full analysis of the data in terms of the refinement of the local gadolinium environment could not be undertaken. However, attempts to fit the data using a simple model with the gadolinium distributed equally over the A1 site (0.5,0.5,0) (8 oxygens at 2.45 Å) and A3 (0.5,0.5,*z*), $z \approx 0.4$, (4 oxygens at 2.79 Å + 4 oxygens at 2.75 Å + 4 oxygen at 2.57 Å) sites produced a very poor fit to the data ($R_{fit} > 50\%$, Figure 5). The poor R_{fit} arises primarily from the region at around 2.8 Å where Gd−O distances are calculated by the ordered model for the A3 site but the experimental data shows little evidence for interactions in this region. The experimental data supports the structure in which distortion of the TiO_6 octahedra modifies the A3 environments producing Gd−O distances of around 2.5 Å or over 3.0 Å. Inputting the refined oxygen positions from the structural model obtained with neutron diffraction data is difficult as the choice of actual oxide ion sites around a gadolinium on an A3 sites would be arbitrary, and several attempts to do so did produce an improvement in the R_{fit}, but this model could not be refined in detail due to the large number of different possible gadolinium to oxygen distances in the 2.5−3.4 Å range.

Results and Discussion

The materials where Ln = Nd, Sm, Eu, and Gd crystallize with a simple quintupled perovskite unit cell of dimensions $1a_p \times 1a_p \times \simeq 5a_p$ essentially containing double layers of CuO_2 separated by triple layers of TiO_6 octahedra, in the primitive tetragonal space group *P*4/*mmm*. For the samarium, europium, and gadolinium samples the distribution of oxygen is consistent with layers formed from CuO_5 square pyramids. However for neodymium, extensive disordering occurs on both the A and B cation sublattices, and there is evidence for the incorporation of oxygen between the CuO_5 pyramids. Similar behavior is seen in the quadruple perovskite system for the larger lanthanides where for lanthanum and neodymium there is strong evidence for the incorporation of oxygen between the CuO_5 square pyramids and disordering occurs on the B cation sublattice.[16,20,21] This behavior is probably associated with the presence of the lanthanide ion between the CuO_5 square pyramids. The separation between the copper atoms in

(19) Binsted, N.; Campbell, J. W.; Gurman, S. J.; Stephenson, P. C. SERC Daresbury Laboratory EXCURV92 computer program, 1992.
(20) Palacin, M. R.; Fuertes, A.; Casañ-Pastor, N.; Gómez-Romero, P. *J. Solid State Chem.* **1995**, *119*, 224; **1995**, *117*, 213.
(21) Greenwood, K. B.; Sarjeant, G. M.; Poeppelmeier, K. R.; Salvador, P. A.; Mason, T. O.; Dabrowski, B.; Rogacki, K.; Chen, Z. *Chem. Mater.* **1995**, *7*, 1355. Otzschi, K. D.; Poeppelmeier, K. R.; Salvador, P. A.; Mason, T. O.; Zhang, H.; Marks, L. D. *J. Am. Chem. Soc.* **1996**, *118*, 8951.

Table 6. Derived Bond Lengths and Angles from Powder Neutron Diffraction (†) and Powder X-ray Diffraction (‡) (PXD) Data for $Ln_2Ba_2CaCu_2Ti_3O_{14}$ (Ln22123)

		distance/Å; angle/deg					
bond		Nd22123†[b]	Sm22123†	Eu22123‡	Gd22123†	Tb22123‡	Dy22123†
Ln(1)−O1	(×8)	2.573(4)	2.490(2)	2.48(2)	2.445(2)	2.45(2)	2.442(4)
Ln(1)−O6	(×1)	2.7602(1)					
Ba(2)−O1	(×4)	2.858(7)	2.895(5)	2.89(3)	2.916(4)	2.91(3)	2.921(7)
Ba(2)−O2	(×4)	2.768(1)	2.772(1)	2.76(1)	2.770(1)	2.75(1)	2.767(1)
Ba(2)−O3	(×4)	2.953(9)	3.085(6)	3.07(4)	3.105(5)	3.04(4)	3.016(9) (×2)
Ca/Ln(3)−O3	(×4)	2.668(8)	2.586(4)	2.60(3)	2.568(4)	2.61(3)	2.274(7) (×2)
							2.721(7) (×2)
Ca/Ln(3)−O4	(×1)	2.42(2)	2.39(1)	2.75(1) (×4)	2.339(8)	2.734(3) (×2)	2.35(1)
	(×2)	2.782(2)	2.775(1)		2.776(1)	2.742(3)	2.64(2) (×1)
	(×1)	3.11(2)	3.11(1)		3.153(8)		2.90(2)
Ca/Ln(3)−O5	(×2)	2.527(8)	2.523(5)	2.786(9) (×4)	2.509(5)	2.79(1) (×4)	2.525(6)
	(×2)	3.11(1)	3.0865(6)		3.119(6)		
Cu−O1	(×4)	1.9522(4)	1.9469(3)	1.946(3)	1.9451(3)	1.940(3)	1.9360(3)
Cu−O2	(×1)	2.34(2)	2.403(9)	2.32(6)	2.414(6)	2.34(6)	2.495(9)
Cu−O6	(×1)[a]	1.64(2)					
Ti(1)−O2	(×1)	1.93(1)	1.912(3)	1.89(6)	1.82(1)	1.90(7)	1.95(2)
Ti(1)−O3	(×4)	1.95(1)	1.951(2)	1.949(5)	1.951(1)	1.942(5)	1.93(1) (×2)
							2.00(1) (×2)
Ti(1)−O4	(×1)	1.88(1)	1.94(2)	2.1(1)	2.08(1)	2.0(1)	1.91(2)
Ti(2)−O4	(×2)	2.09(1)	1.970(7)	1.86(10)	1.922(7)	1.9(1)	1.96(1)
Ti(2)−O5	(×4)	1.996(2)	1.988(2)	1.941(1)	1.989(2)	1.935(1)	1.97(2) (×2)
							1.99(2) (×2)
Cu−O1−Cu		177.6(10)	175.7(4)	171.9(21)	171.3(3)	171.9(25)	175.8(5)
Ti(1)−O3−Ti(1)		175.6(4)	171.5(13)	169.9(32)	167.1(6)	171.0(4)	159.2(6)
O1−Cu−O1		89.98(2)	89.92(1)	86.5(9)	89.67(2)	89.9(2)	89.71(2)
O3−Ti1−O3		89.92(2)	89.69(9)	89.6(3)	89.28(6)	89.8(3)	88.9(2)
						89.5(3)	89.9(2)

[a] 0.32(3) occupied site. [b] For neodymium the bond description given in the left-hand column represents the A site occupancies as summarized in Table 4.

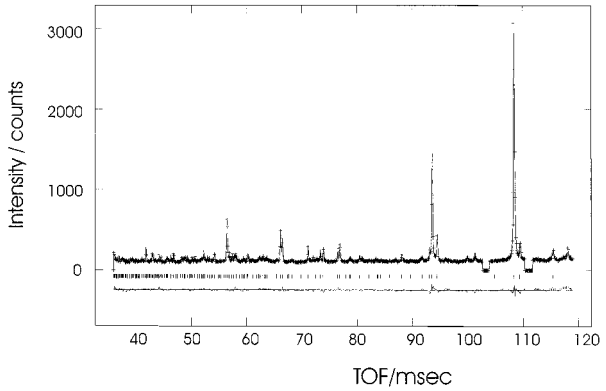

Figure 3. Fit to the powder neutron diffraction data from $^{160}Gd_2Ba_2CaCu_2Ti_3O_{14}$. Experimental data points are shown as crosses, calculated profile the upper continuous line, and difference profiles as the lower continuous line. Tick marks show reflection positions. Time-of-flight (ms) can by converted to *d* spacing (Å) by division by 48.26.

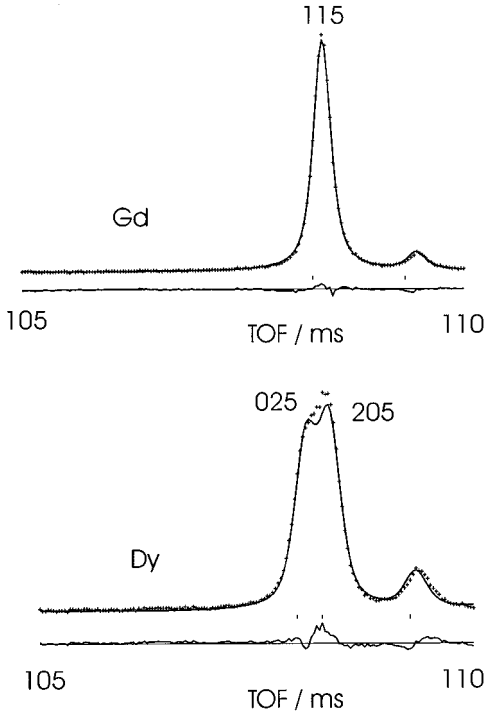

Figure 4. Portion of the fit to the powder neutron diffraction profile from $Dy_2Ba_2CaCu_2Ti_3O_{14}$ in comparison to that from $Gd_2Ba_2CaCu_2Ti_3O_{14}$ in the same region showing the reduction in symmetry to orthorhombic.

these layers is of the order of 3.25 Å in these materials, and while the heavier and smaller lanthanides frequently adopt coordination numbers as low as eight, the larger lanthanides prefer higher coordination numbers. Local incorporation of oxygen between the CuO_5 blocks satisfies this requirement. For the largest trivalent ion studied, lanthanum, this disordering of the A and B cations becomes complete leading to a simple cubic perovskite cell.

For all compositions the central TiO_6 octahedron is distorted and/or tilted; this model is supported by the refined atomic coordinates and also the EXAFS experiment. Again this is similar behavior to that observed in the quadruple perovskites with tin and titanium octahedra separating the copper units. The origin of this distortion seems to lie in the mismatch between the sizes of the copper oxygen bond length, ideally 1.96 Å in CuO_2 square planes, and the titanium oxygen distances, typically 2.02 Å in TiO_6 octahedra. Without tilting the in-plane Ti−O distances would be compressed unsatisfactorily to values similar to the Cu−O distance, roughly half the *a* lattice parameter. With disordering of the oxygen and tilting, the in-plane Ti−O values

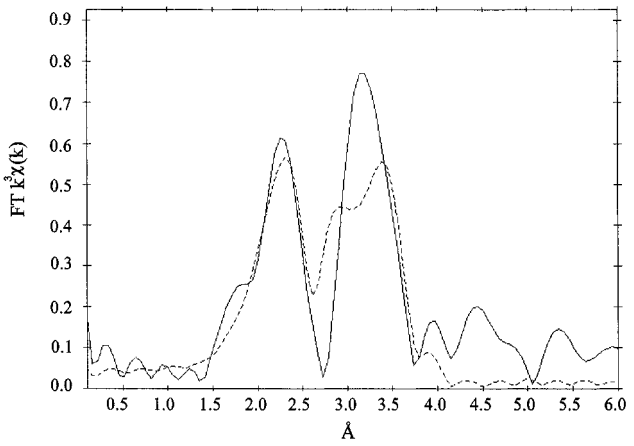

Figure 5. Fit to the Fourier transform of the Gd L III edge data from $Gd_2Ba_2CaCu_2Ti_3O_{14}$ using an ordered oxide model. Dotted line, theory; continuous line, experimental.

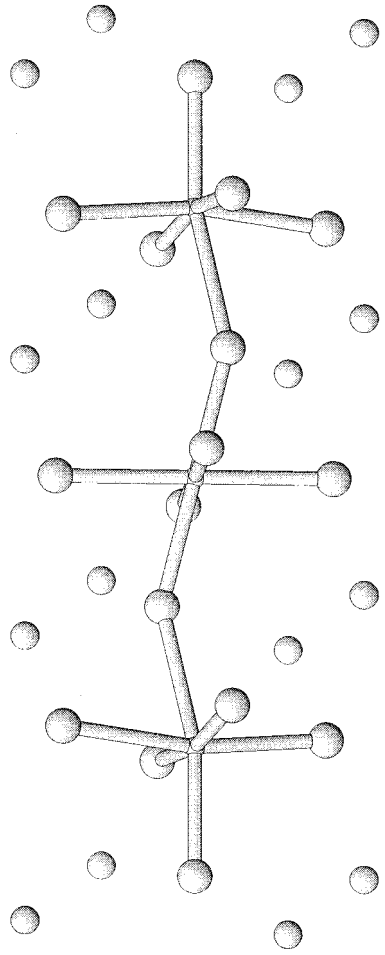

Figure 6. Schematic view of the distortion/tilting of the TiO_6 octahedra in the $Ln_2Ba_2CaCu_2Ti_3O_{14}$ structure.

around Ti(2) average about 0.03 Å longer than the values that would be obtained for regular octahedra. However, other factors may also contribute to the distortions found in this structure, for example, the general tendency of titanium to adopt nonperfect octahedral geometries and the coordination preferences of the lanthanide ions. Titanium is frequently found in distorted octahedral environments, for example, $BaTiO_3$ and $Bi_2TiO_4F_2$, and the geometry refined in these quintuple perovskites around the titanium is similar. Figure 6 shows a likely geometry for the three TiO_6 octahedra, though with the use of disordered positions

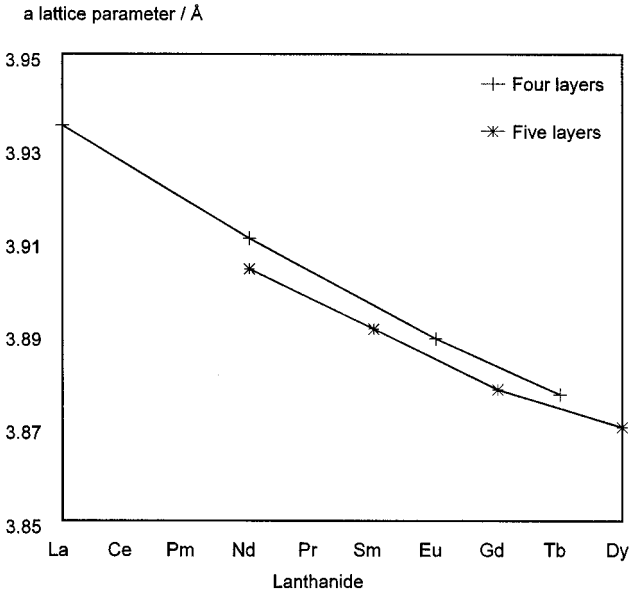

Figure 7. Variation in the *a* lattice parameter of the quadruple and quintuple perovskites as a function of lanthanide.

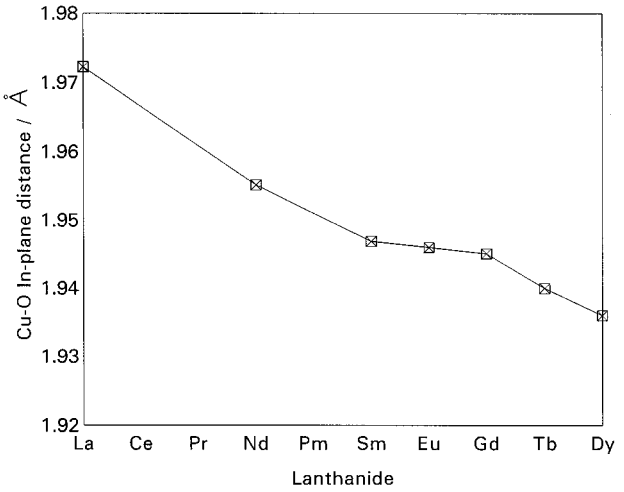

Figure 8. Variation of the Cu−O distance in the quintuple perovskites as a function of lanthanide size. For $Dy_2Ba_2CaCu_2Ti_3O_{14}$ and $Tb_2Ba_2CaCu_2Ti_3O_{14}$ an average value are given.

in the refinement this represents just one possibility. This tilting also changes the coordination to the A cations, particularly A3, which is occupied by both the lanthanide and calcium. Concerted tilting of the octahedra may permit better coordination for specific sites containing either calcium (12-fold coordination $r(Ca^{2+}) = 1.34$ Å) or the distinctly smaller Ln^{3+} (e.g., $r(Sm^{3+}) = 1.24$ Å). Such a concerted tilting of the octahedra is supported by the EXAFS data, which support a structure in which the lanthanide environment is shifted away from a near-regular 12-fold coordination to oxygen. The degree of ordering of the A cations is also observed to increase with decreasing lanthanide size, essentially being perfect for samarium.

For the smallest lanthanides studied, terbium and dysprosium, the structure undergoes a further increase in structure complexity. $Dy_2Ba_2CaCu_2Ti_3O_{14}$ crystallizes with a quintupled perovskite type unit cell of approximate dimensions $\sqrt{2}a_p \times \sqrt{2}a_{p'} \times \simeq 5a_p$ with $a_p \approx a_{p'}$ in the orthorhombic space group *Cmmm*. This doubling of the area of the basal plane is seen in many super-

conductor and superconductor related phases, such as $Pb_2Sr_2YCu_3O_8$[17] and La_2CuO_4. In the quintupled perovskite structure the formation of the orthorhombic cell probably allows better coordination between oxygen and the A type cations, with shorter but fewer interactions, when the lanthanide ion size is reduced.

Attempts to dope the *quadruple* perovskite structure in order to raise the copper oxidation state above 2 and induce superconductivity have met with little success.[16,20,21] Certainly the system is extremely difficult to dope, though replacement of titanium by copper seems feasible. However, in the quadruple perovskites the in-plane Cu−O distance remains relatively long for a superconducting phase where distances of the order of 1.95 Å or less are normal. Reduction in the lanthanide size in the quadruple perovskites goes some way to addressing this problem, but even for Ln = Tb the value for the Cu−O distance is 1.947 Å.[16,20]

As with the four-layer materials, for the quintuple perovskites a clear trend is observed in lattice parameters as a function of lanthanide size (Figure 7). With little change in the planarity of the CuO_2 structural feature the Cu−O bond distance is observed to decrease with the lanthanide ionic radii falling to 1.945 Å for gadolinium and an average of 1.936 Å for dysprosium (Figure 8), similar to that found in many cuprate superconductors. In terms of the geometry of the CuO_2 planes, the quintuple perovskites therefore exhibit all the structural features of high-temperature superconductors. Doping studies are in progress with the aim of increasing the oxidation state of copper above 2, though even this may not induce superconductivity as the separation of the CuO_2 layers, approximately 16 Å, is larger than in any known superconducting phase.

Acknowledgment. We thank the EPSRC for grants in support of this work and studentships for A.G. and M.J.P. We also thank the EPSRC and DRAL for the provision of neutron beam and synchrotron.

CM960575O